Supplemental information

Dual Immunostimulatory Pathway Agonism through a Synthetic Nanocarrier Triggers Robust Anti-Tumor Immunity in Murine Glioblastoma

Sophie Lugani[1,2]*, Elias A. Halabi[1]*, Juhyun Oh[1], Rainer Kohler[1], Hannah Peterson[1], Xandra O. Breakefield[3,4], E. Antonio A. Chiocca[5], Miles A. Miller[1], Christopher Garris[1#], Ralph Weissleder[1,3,5,6#]

* equal contributions

[1] Center for Systems Biology, Massachusetts General Hospital, 185 Cambridge St, CPZN 5206, Boston, MA 02114

[2] Medical Faculty, Heidelberg University, Im Neuenheimer Feld 672, 69120 Heidelberg

[3] Department of Radiology, Massachusetts General Hospital, and Harvard Medical School, Boston, MA

[4] Department of Neurology, Massachusetts General Hospital, and Harvard Medical School, Boston, MA

[5] Department of Neurosurgery, Brigham and Women Hospital, and Harvard Medical School, Boston, MA

[6] Department of Systems Biology, Harvard Medical School, 200 Longwood Ave, Boston, MA 02115

#Ralph Weissleder, MD, Ph.D. (contact)
Center for Systems Biology
Massachusetts General Hospital
185 Cambridge St, CPZN 5206
Boston, MA, 02114
617-726-8226
rweissleder@mgh.harvard.edu

Fig. S1. Synthesis and characterization of CANDIs. A. Schematic depiction of the synthesis, fluorescent labeling and loading of selected therapeutic payloads (LCL-161 & R848) in CANDIs. **B.** CANDI study groups (controls top, therapies bottom). **C.** Dynamic light scattering (DLS) measurement of the hydrodynamic diameter of CANDI with an average size of d = 27± 4 nm (N = 3) and zeta potential measurement of the surface charge of CANDI with an average charge of ζ = -9.56 mW (N = 3), measured in PBS (0.01x). **D.** Normalized absorption and emission spectra of CANDI, CANDI-PB (blue) & CANDI-AF647 (orange) depicting excitation and emission maxima (λ_{ex}, λ_{em}, PBS 1x, N = 3).

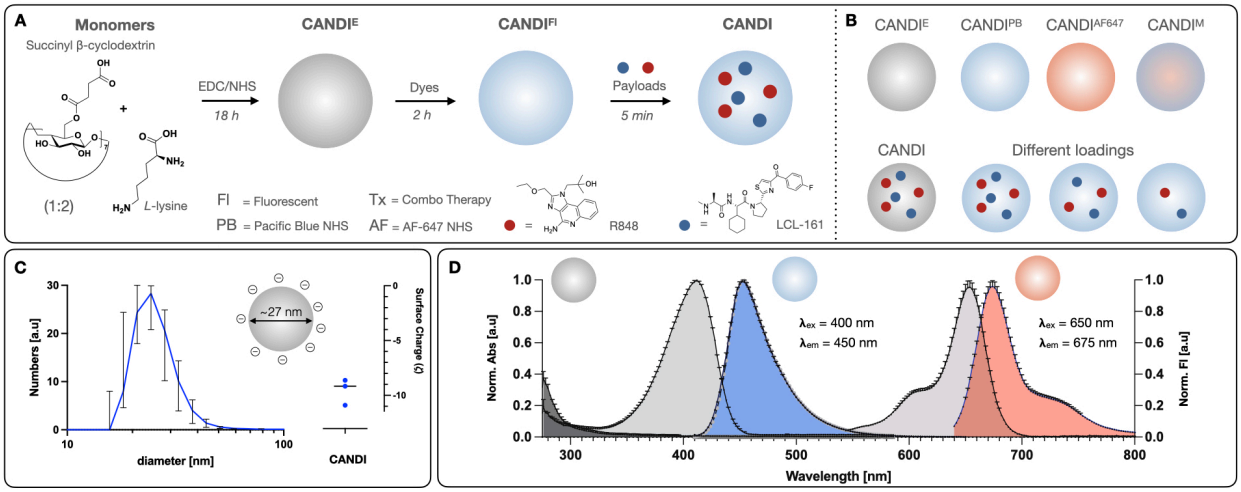

Fig. S2. **Loading and release kinetics of CANDIs**. **A**. Schematic depiction of loading experiments using phenolphthalein as indicator (**P**, pH = 10.5). In its deprotonated form, **P** exhibits high absorption at 550 nm (λ_{max}). Upon interaction with the cyclodextrin (CD) units contained in/on the CANDI, **P** undergoes a spirocyclization depleting its absorbance (**P**→No drug). Signal recovery is obtained by displacement of the indicator P by addition of i) R848 alone (0.2 mg) 21.14%, ii) LCL-161 alone (0.5 mg) 57.60% and iii) R848 (0.2 mg) plus LCL-161 (0.5 mg), 85% (N = 3, P = 0.0068). **B**. Release experiments determined by DLS measurements comparing unloaded CANDI (solid black line) to a loaded CANDI (blue, payloads) at a loading concentration of 5 mg CANDI in 100 µL PBS. An increase in size of d ~10 nm is evident upon loading. Release of the loaded payloads and shrinking of CANDI to its unloaded size (orange) was achieved after 24 h dialysis (3k, PBS, 0.01x) and statistical analysis of the mean distribution of particle size (N = 3, P = 0.0047). **C.** Standard curve to estimate payload concentration from ELSD signal intensity (left) and release kinetics of R848 and LCL-161 with an estimated half-life of 0.5 ± 0.32 h and 1.4 ± 0.5 h h and ~77% and 78% release respectively after membrane filtration assays in PBS at 37 °C for 18 h (N =

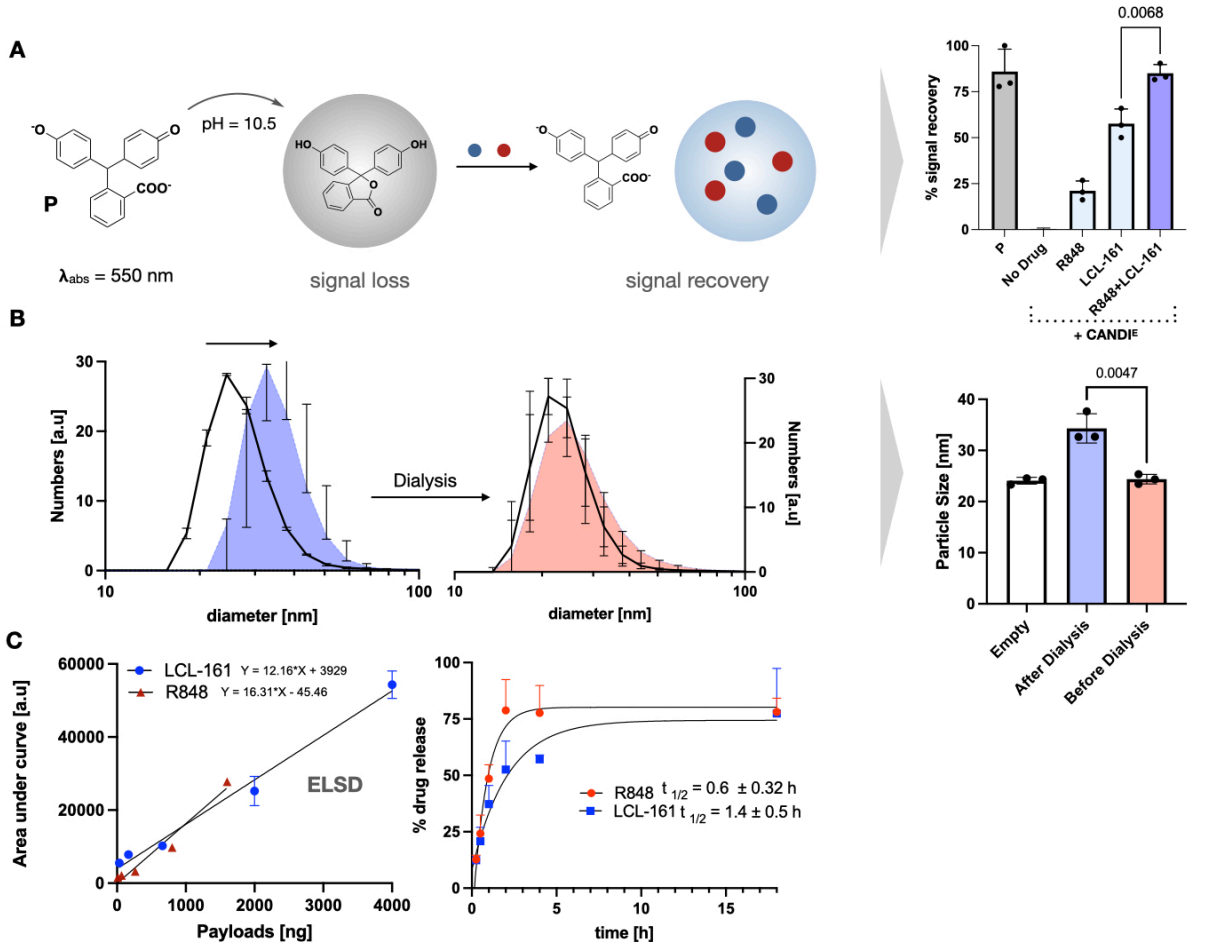

3).

Fig. S3. Additional characterization of CANDI. A. Scanning electron microscopy images of CANDI-tx coated in a ~8 nm gold layer (Scale bars = 10 µm left, and 100 nm right). **B**. Nanoparticle tracking analysis of CANDI^{E} and CANDI solutions showing size distributions, homogeneity, and estimated particle concentration for in vivo dose. Scale bars for panel A = 10 µm (left) and 100 nm (right). **C**. Transmission electron microscopy images of CANDI negative stained with uranyl acetate (Scale bar = 50 nm).

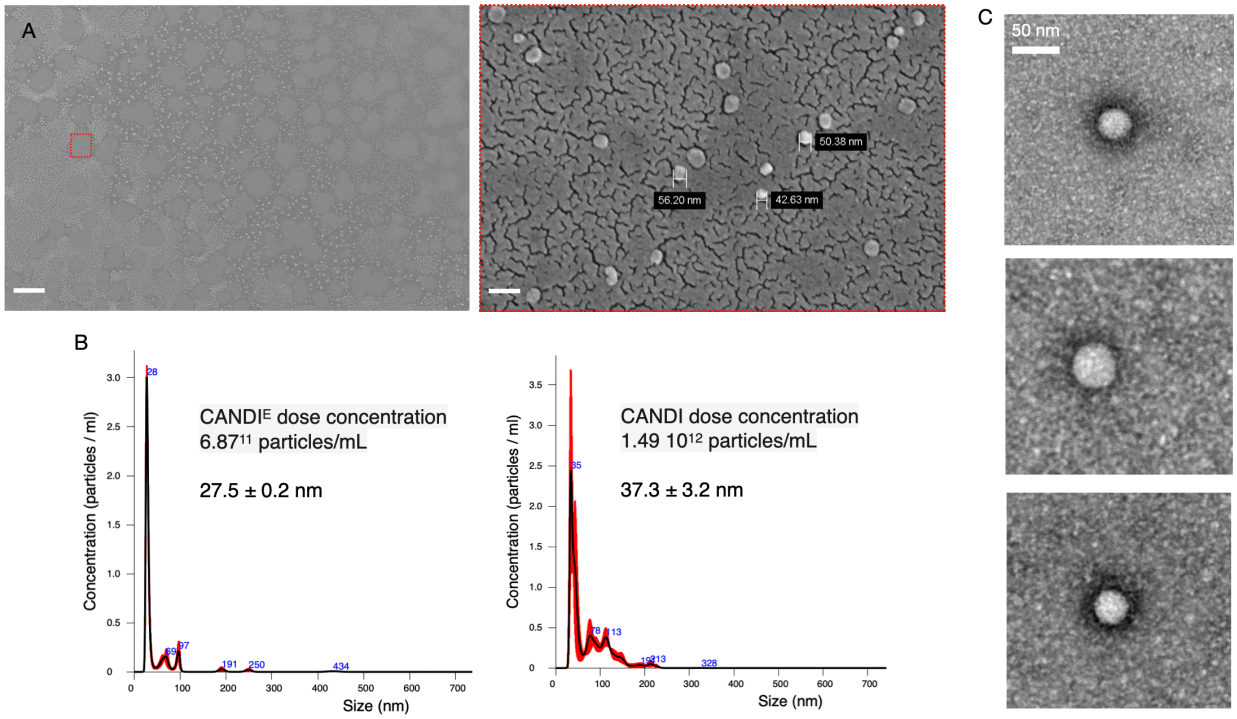

Fig. S4: X-ray photoelectron spectroscopy analysis of CANDI^{E} and CANDI. A. survey scans confirm the presence of S and F atoms in the loaded CANDI and **B**. C 1s narrow scan exhibits enhanced aliphatic and aromatic binding energies correlating to the loaded payloads.

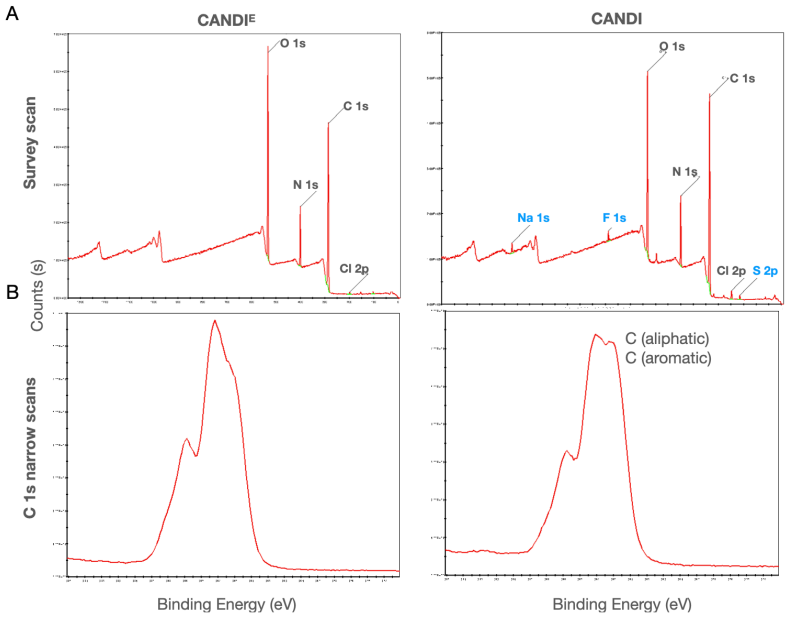

Atom	CANDIe Atomic %	CANDI Atomic %
C (1s)	61.73	63.39
O (1s)	26.91	21.93
N (1s)	10.83	11.08
Cl (2p)	0.23	1.49
Na (1s)	-	1.02
S (2p)	-	0.62
F (1s)	-	0.2

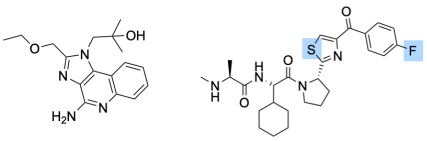

Fig. S5: Attenuated total reflectance (AFT) Fourier-transform infrared spectroscopy (FTIR) comparison of CANDI^{E} vs CANDI. The spectral mathematical correction, revealed absorbance bands that correlate to the vibrations of functional groups contained in each loaded payloads (R848 and LCL-161).

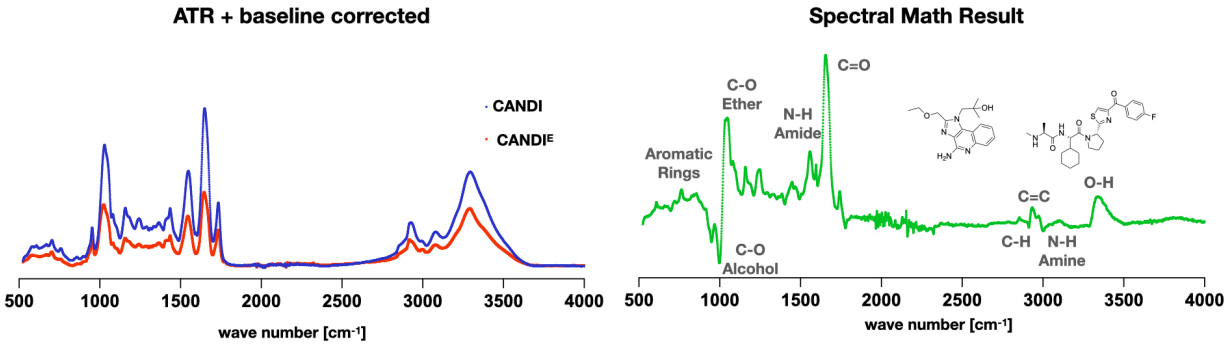

Fig. S6: ^{1}H-NMR spectra in D_2O. A. CANDI^E (5 mg) and **B.** CANDI (5 mg) loaded with a 1:1 mixture of LCL-161 and R-848. The zoomed-in aromatic region of the 2D COSY-NMR spectrum indicates the coupling between the aromatic protons and allows the identification of each aromatic proton respective to the loaded drugs (red numbers). The integrals of each peak confirm a 1:1 mixture of the solubilized drugs, suggesting that both drugs can form complexes with the CD units of the CANDI that make them soluble in D_2O. **C**. Turbidity experiments of payload solution (6 mM, PBS) dissolved in 5 mg CANDI (left) and the same solution without CANDI (right) showing colloidal dispersion and aggregation of the payloads in the absence of the CANDI vehicle.

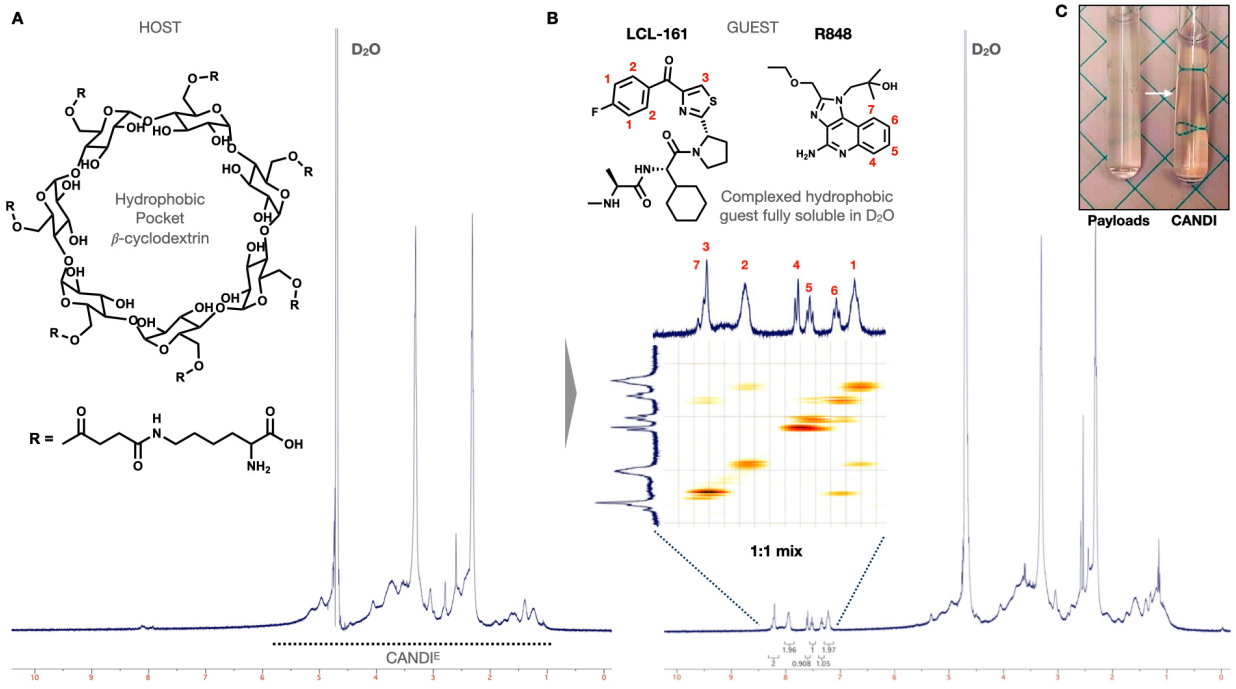

Fig. S7: Characterization of the loaded drugs by liquid chromatography and mass spectrometry (LC-MS). **A**. (Top) Chromatogram (water + acetonitrile with 0.1% formic acid) of a 2:3 mixture of reference compounds R848 and LCL-161 respectively in DMSO. Retention times for R848 and LCL-161 were t = 0.49 min and 0.8 min, respectively. (Bottom) Chromatograms of the unloaded CANDI (black) vs. loaded CANDI with R848 and LCL-161 (red). A relative shift in the retention time of the CANDI was observed, possibly due to complexation with the hydrophobic drugs. The retention times of the complexed drugs matched those of the reference run. The identity of the loaded drugs was also characterized by **B**. their mass-to-charge ratio (ES^+) M^+ = 315 and 501 and C. absorbance spectra for the respective peaks (* & **) obtained from the LC-MS chromatogram in panel A.

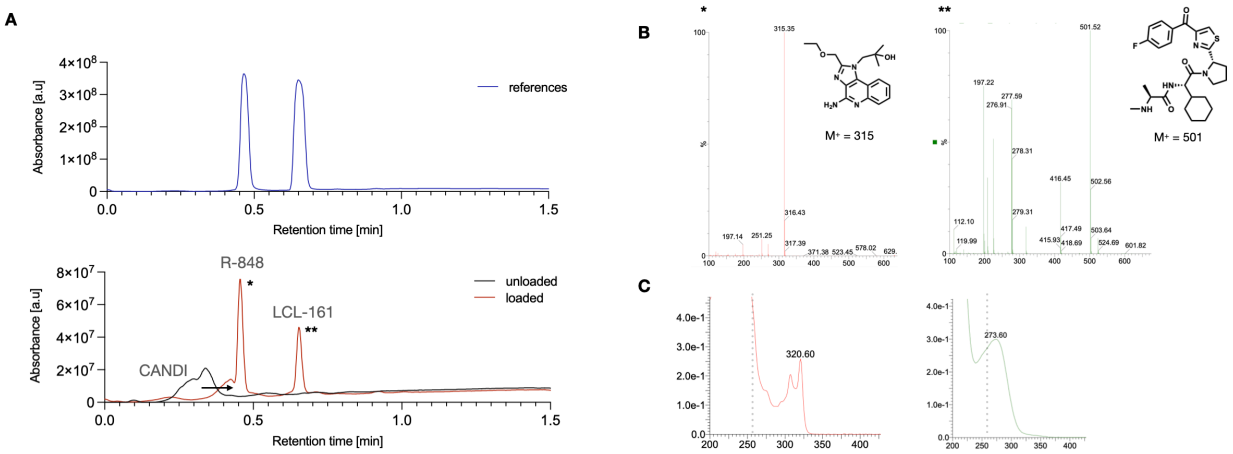

Fig. S8: Effect of CANDI dose on the cellular accumulation in window chamber model. All CANDI^{AF647} doses were given IV, and the tumor microenvironment was imaged 24 h later (scale bar = 50 μm). Images in each row have the same window and level setting. Note that cellular accumulation occurs even at very low doses (doses are given per mouse, i.e., 1 mg = 40 mg/kg).

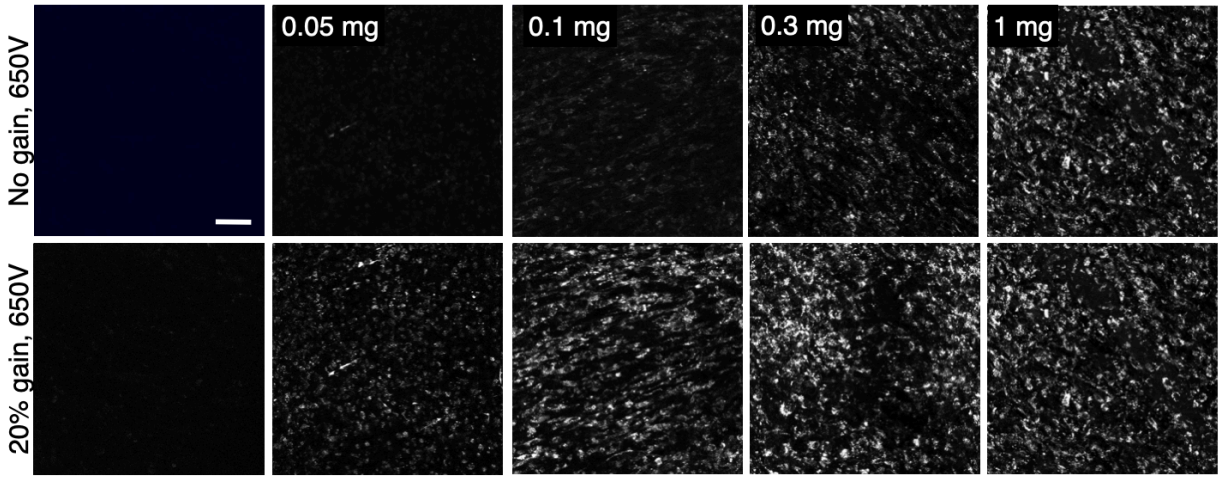

Fig. S9: Brain-tumor distribution of CANDI. Low magnification fluorescence images of resected brains (green autofluorescence) containing CT2A tumors (red) and CANDI^{AF647} (white). Merge represents a combination of the CANDI and CT2A channels. Note the high tumoral accumulation of CANDI. Scale bar = 2 mm.

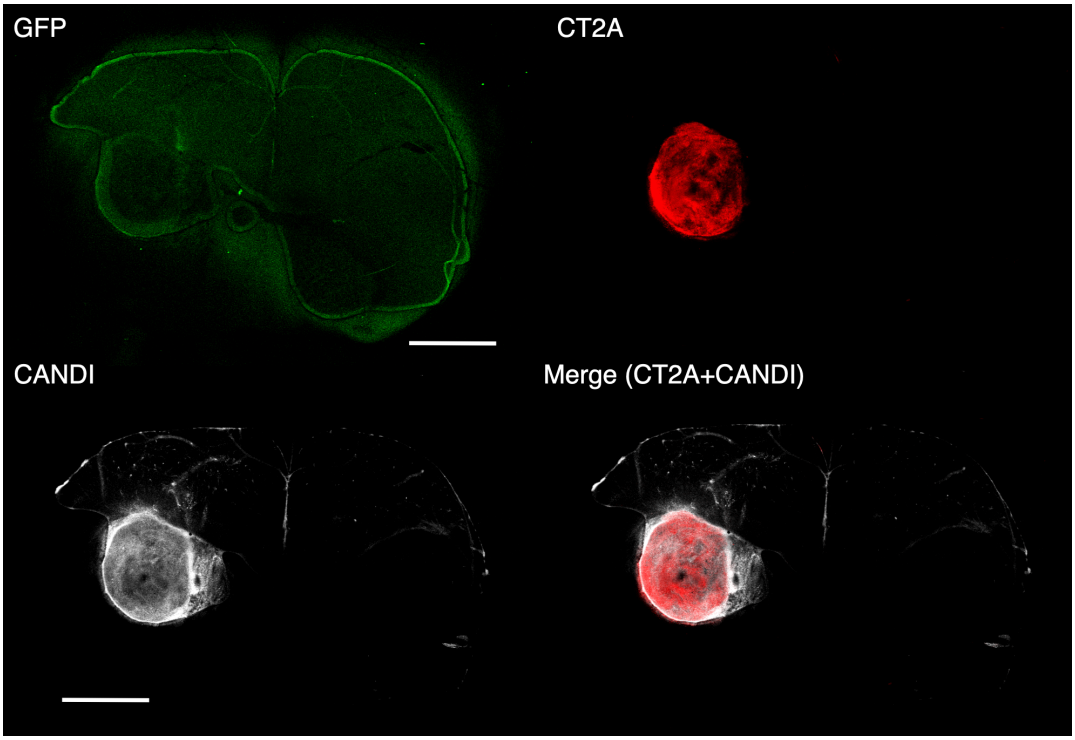

Fig. S10: Flow cytometry of tissues with highest CANDI accumulation. Tissues were isolated from mice treated with CANDI^{AF647} and processed into single-cell suspensions for flow cytometry analysis. Data are expressed as mean fluorescent intensity of AF647 in each respective cellular population indicated. **A**. GBM CT2A (N = 4) **B**. cervical lymph node (N = 3). Note the increased uptake of CANDI into macrophage and DC subtypes.

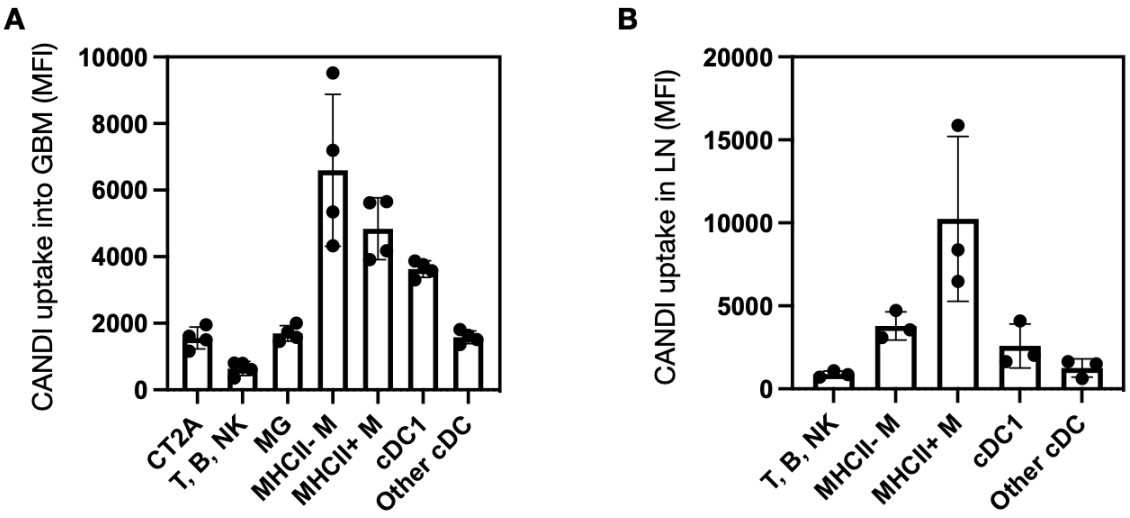

Fig. S11: Multiplexed FAST cycling method used for tissue analysis. A. Frozen tumor sections were incubated with FAST-reagent labeled antibodies, quenched, and then restrained for multiple cycles. Image analysis was performed on multiple filed of view from multiple animals (for data, see **Fig. 8**). **B**. Schematic diagram of the TCO containing FAST linker between a given antibody and the fluorochrome. The TCO allowed efficient quenching of the affinity ligands once bound to tissue. For ESI-MS and ^{1}H NMR of the linker and BHQ3-Tz, see[63].

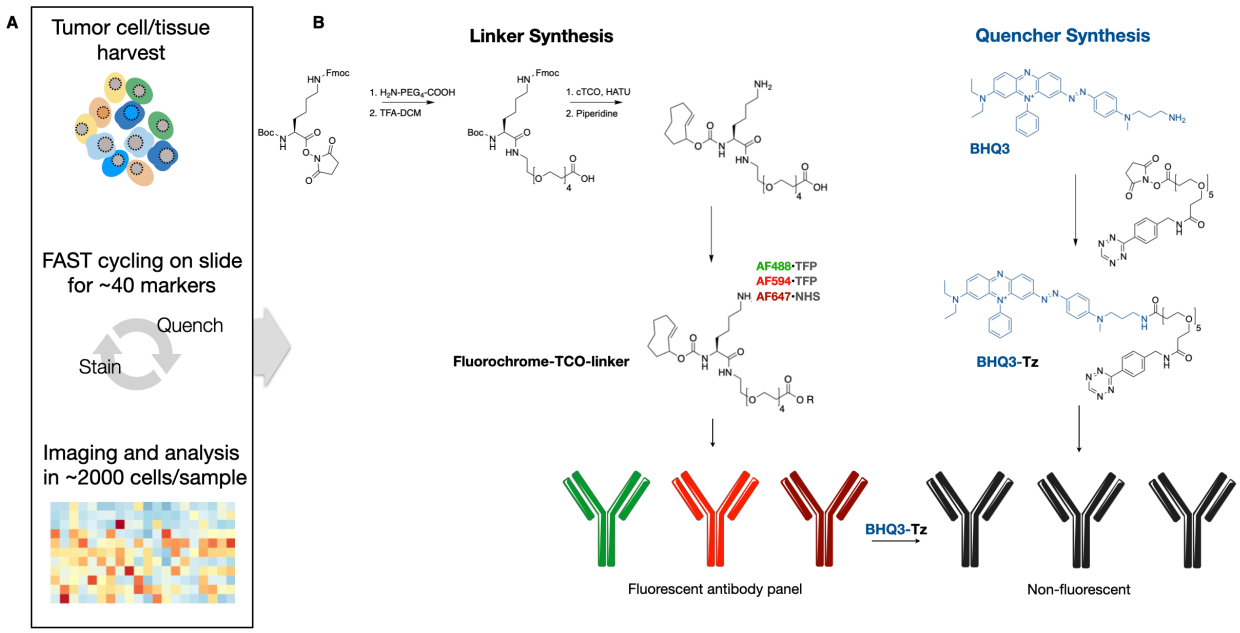

Fig. S12: CANDI-uptake by tumor-associated immune cells. **A**. Merged images of the CANDI signal (white, top) and the immune cell staining in **Fig. 6A** are shown (bottom). Cyan: TMEM119, green: CD11c, red: F4/80, magenta: GFAP. **B**. Another example of CANDI (white) uptake in different immune cell populations (green) in CT2A tumor (blue).

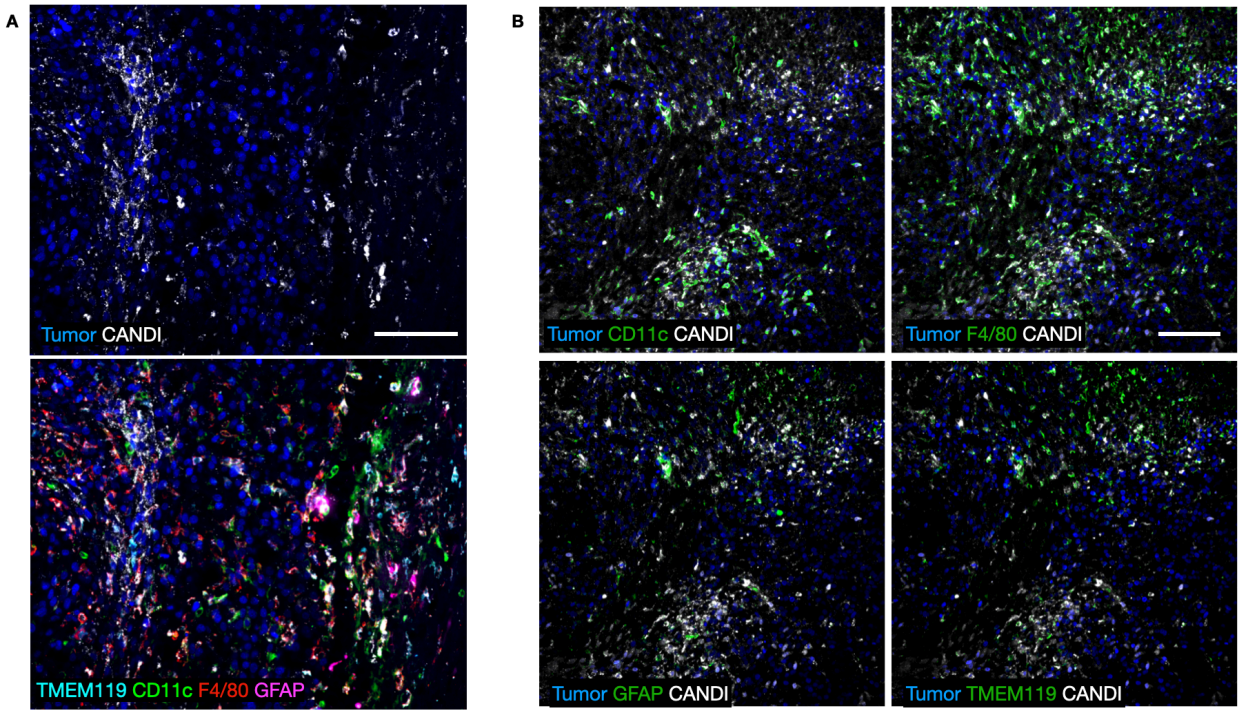

Fig. S13: Bioluminescence imaging of treatment effects. CT2A tumor-bearing mice were imaged by bioluminescence following IV administration of 5 mg of luciferin. Shown are six representative mice from the three treatment cohorts. For additional MR imaging, see **Fig. S12**.

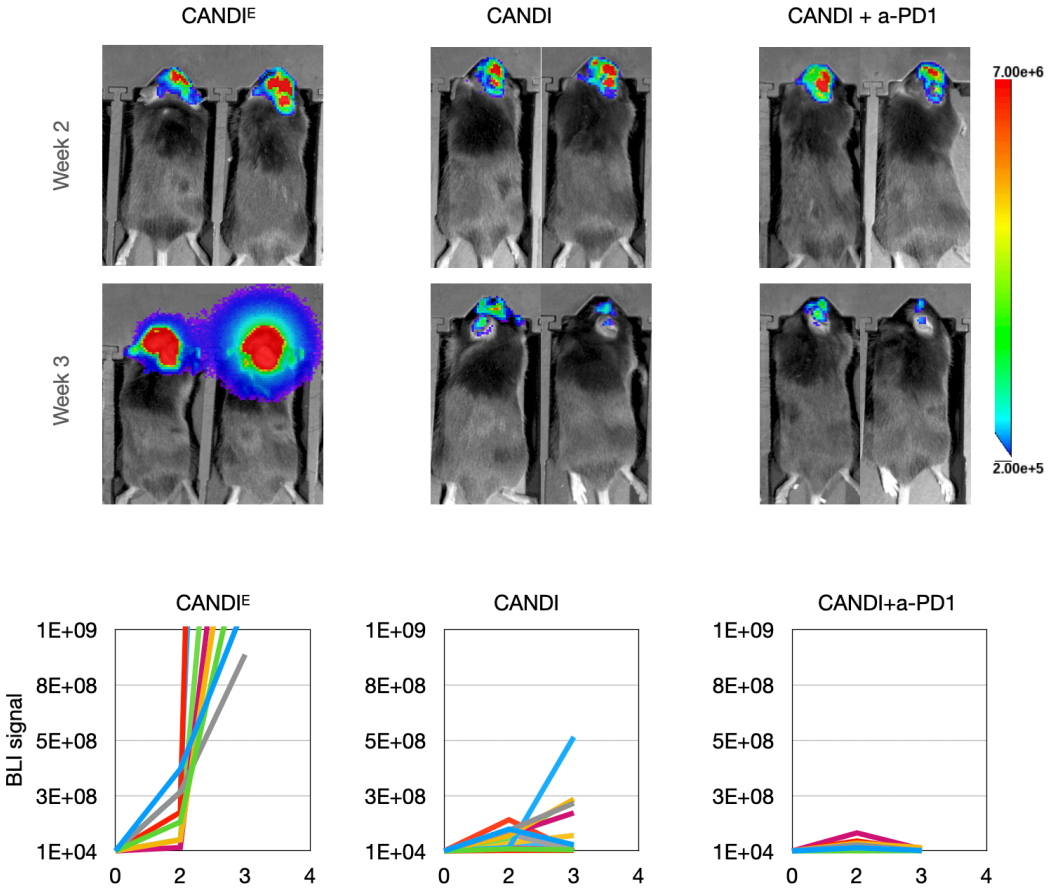

Fig. S14: MR imaging of treatment effects. T1W (± Gd) and T2 weighted MR images were obtained in 9 mice at weeks 2 (before treatment) and at week 3 after two treatments with either CANDI^{E}, CANDI, or CANDI + a-PD1. Note the marked tumor differences in the latter cohort.

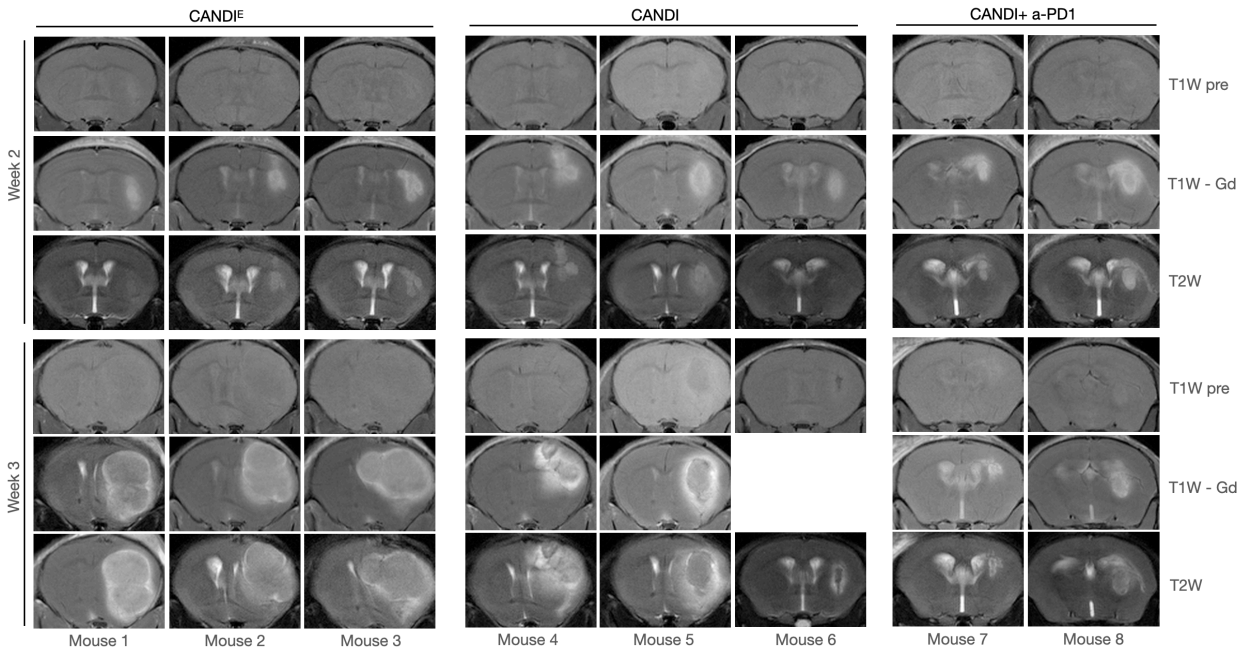

Fig. S15: Toxicity. A. There is no significant adverse effect of drug-loaded CANDI on body weight, unlike other immunostimulatory drugs (e.g., STING agonists). Tumor-bearing mice treated with a therapeutic dose of CANDI (N = 24). **B**. Effect of CANDI treatment on liver histology (representative images from mice injected with either CANDI or CANDI^{E}, N = 10). Note the typical architecture and lack of vacuolization or immune cell infiltrates.

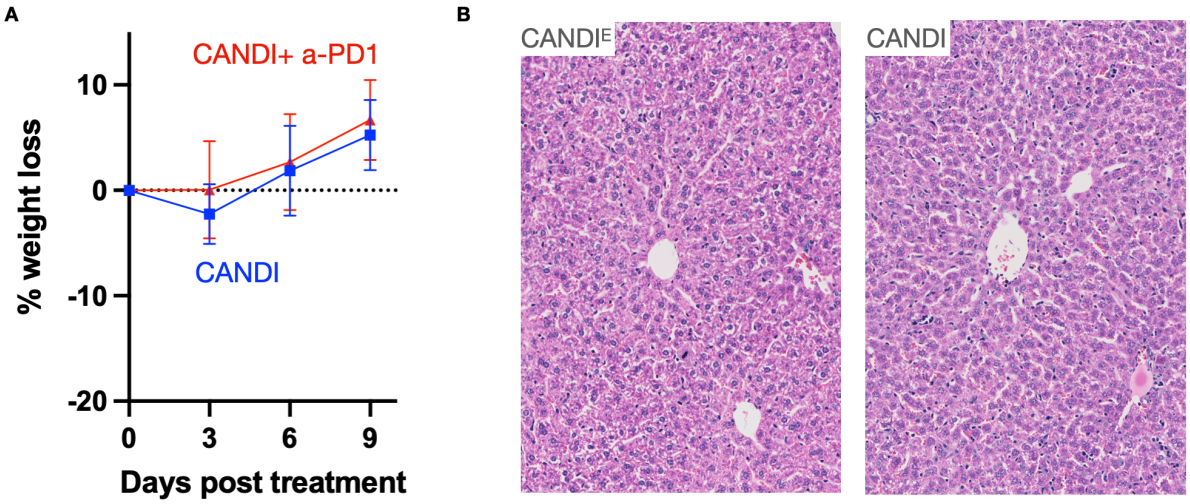

Fig. S16: Effects of CANDI on IL-12 expression in GBM. Intravital imaging was performed in the CT2A brain window model (red) of IL-12-eYFP reporter mice receiving CANDI (white). The top row shows CANDI distribution 2, 24, and 48 h after IV administration. The bottom row shows the IL-12 induction. After CANDI administration, many more cells are green in the tumor microenvironment. While both cell types can express IL-12, DC generally express more IL-12 than MF, however, DC are far less numerous in the tumor microenvironment compared to MF. Shown is one representative example of N = 6 mice tested; scale bars = 100 μm.

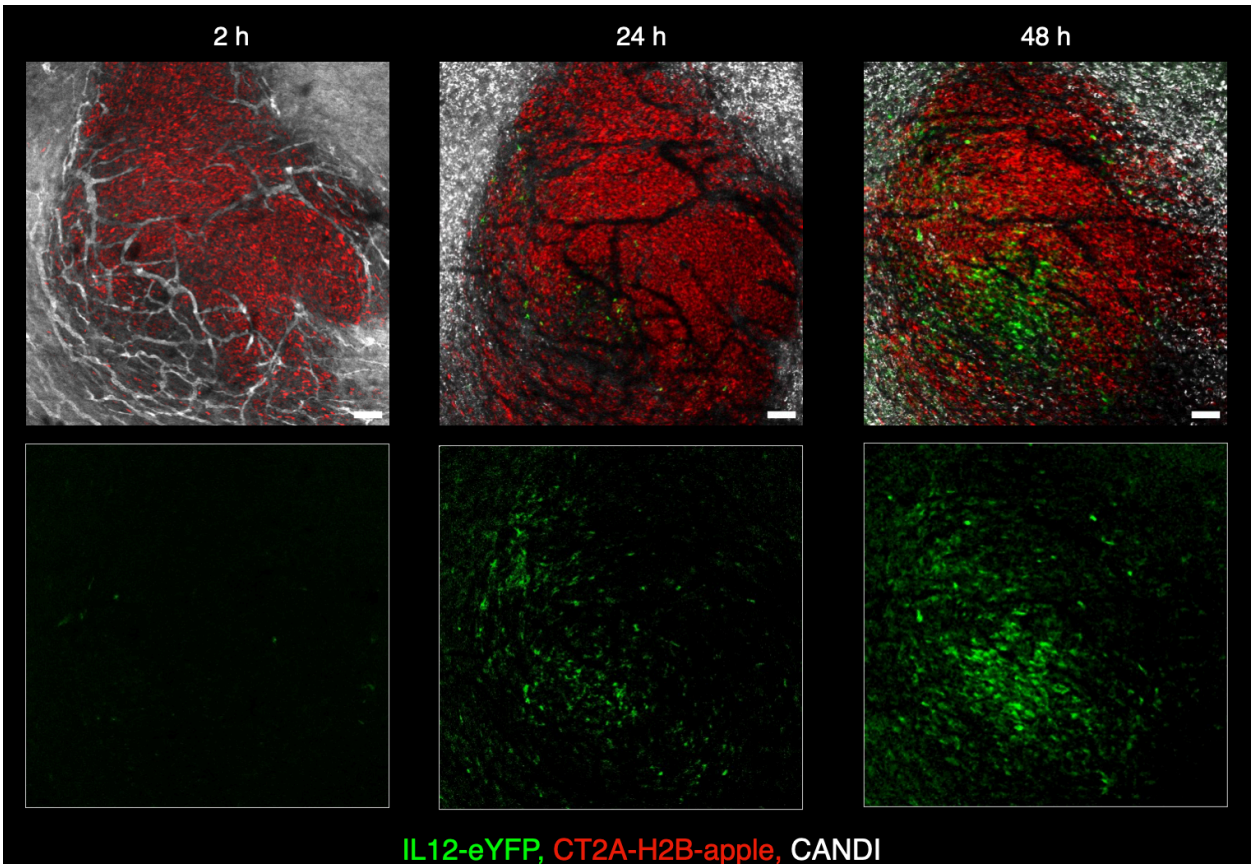

Fig. S17: Effects of CANDI on IFNG expression in GBM. Intravital imaging was performed in the CT2A brain window model (red) of IFNG-eYFP reporter mice (GREAT mice) receiving CANDI (white). The top row shows tumor growth. The bottom row shows CANDI distribution 24, 48, 72, and 96 h after IV administration. The middle row shows the IFNG induction. Note that many more cells are green in the tumor microenvironment after 96 days following CANDI administration. Shown is one representative example of N = 5 mice imaged; scale bar = 50 μm. See **Movie 4** for longer time course and cell mobility.

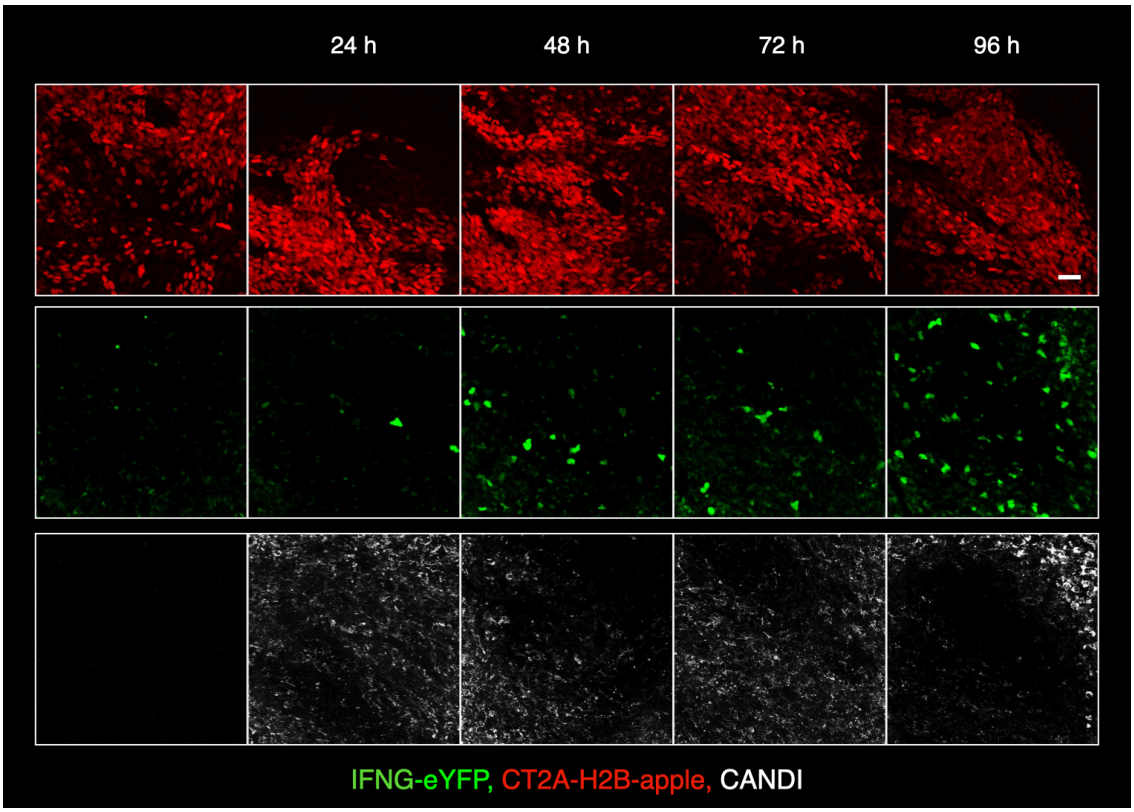

Fig. S18: Modeling. Systemic PK parameters were modeled to determine the relative advantages of CANDI complex small molecules for TAM delivery. The data was fit to published clinical blood PK data as detailed in **Tables S4**. As can be seen, CANDI encapsulation resulted in approximately 6 orders of magnitude higher tumoral concentrations of the small molecules at 1 day after systemic administration, and local drug concentrations remained stable for prolonged times.

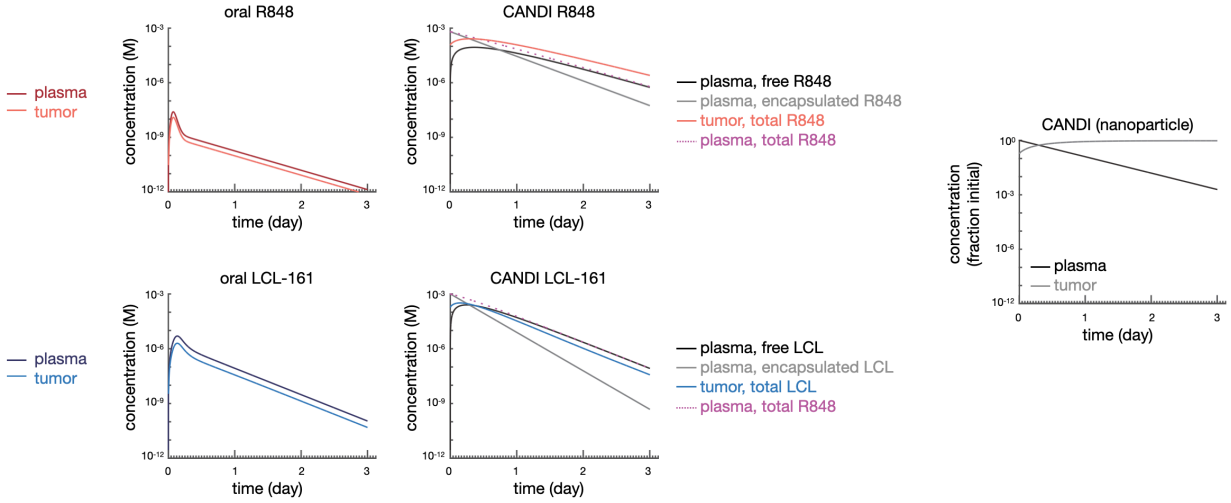

TABLES

Table S1: FAST reagents for murine cyclic immunostaining

Markers	Target population	Clone	Source	Catalog #	Dye
CD45	Hematopoietic cells	104.2	Bio X Cell	BE0300	AF488
CD3	T cells	145-2C11	Biolegend	100322	AF647
CD8	CD8+ T cells	53-6.7	Biolegend	100702	AF647
CD4	CD4+ T cells	RM4-5	Biolegend	100505	AF488
TMEM119	Microglia	28-3	Abcam	AB209064	AF647
F4/80	Macrophages	CI:A3-1	Bio X Cell	BE0206	AF488
CD11b	Myeloid cells	M1/70	Bio X Cell	BE007	AF647
CD11c	Dendritic cells	N418	Biolegend	117302	AF647
MHCII	Various	M5/114	Bio X Cell	BE0108	AF488
PD-L1	Various	Polyclonal	R&D	135229	AF488
IL-12	Various	45806	R&D	MAB6688	AF488

Table S2: Antibodies for murine flow cytometry

Markers	Target population	Clone	Source	Catalog #	Dye
Sirpα	Myeloid cells	P84	Thermo Fisher	64-1721-80	SB645
CD40	Antigen Presenting Cells	3/23	Biolegend	124626	Pacific Blue
CD86	Antigen Presenting Cells	GL-1	Biolegend	105043	BV785
CD3e	T cells	145-2C11	Thermo Fisher	15-0031-81	PE-Cy5
CD19	B cells	1D3	Thermo Fisher	15-0193-81	PE-Cy5
B220	T cells	RA3-6B2	Thermo Fisher	15–452-81	PE-Cy5
NK1.1	NK cells	PK136	Biolegend	108716	PE-Cy5
XCR1	Dendritic cells	ZET	Biolegend	148204	PE
CD11c	Dendritic cells	N418	Thermo Fisher	61-0114-82	PE-eF610
CD45	Hematopoietic cells	30-F11	Thermo Fisher	56-0451-82	AF700
MHCII	Antigen Presenting Cells	M5/114.15.2	Thermo Fisher	47-5321-82	APC-eF780
PD1	Various	RMP1-14	Biolegend	114117	PE
CD3e	T cells	145-2C11	Biolegend	100349	Bv711
CD8α	CD8+ T cells	53-6.7	BD Biosciences	557668	AF488
CD4	CD4+ T cells	RM4-5	BD Biosciences	558107	Pacific Blue
CD11b	Myeloid cells	M1/70	BD Biosciences	557397	PE

Table S3: Comparison of some carbohydrate based therapeutics with TAM targeting capabilities

Table S3: Comparison of carbohydrate based therapeutics with TAM targeting capabilities

Nanomaterial	Polymer	Target cell	Size (nm)	Payload (mg drug)/ mg polymer	Payload type	TAM localization	Therpeutics efficacy	Reference
CANDI	B-CD	DC + TAM	37 ± 3.2	0.14	Dual and triple	>500% ID/ g	GBM, some complete	This work
CDNP	Cyclodext rin	TAM	~30	0.12	TLRa	90% ID/g	Flank tumor, growth retardation	Nat Biomed Eng, 2018;2: 578
Macrin	Dextran	TAM	~20	20 molecules/ NP	Chelator	20% ID/g	Not tested	*ACS Nano*. 2018; 12 12015
Ferumoxytol	Dextran	TAM	17-31	12 molecules/ NP	Peptides			Nano Lett, 2017;17: 7160
Ferumoxytol	Dextran	TAM	17-31	~100 molecules/ NP	Taxol, Doxorubici n		Growth retardation	Nat Comm. 2014:5:338 4
CHP:LPA	Pullulan	TAM	~40	~0.03	Long peptide antigen (LPA)		Flank tumor sensitized to adaptive immune	J. Clin. Invest;2019 ;129;1278

Tables S4: Pharmacokinetic parameters used for modeling. For references see[34–36,65,66]

Parameter	LCL-161 single agent	Notes
Dose	25 mg/kg	J Clin Oncol. 2014;32(28):3103-3110.
C_{max}	2,350 ng / mL	J Clin Oncol. 2014;32(28):3103-3110.
AUC_{plasma}	32,081 ng hr / mL	J Clin Oncol. 2014;32(28):3103-3110.
$t_{1/2\ terminal}$	5 hr	J Clin Oncol. 2014;32(28):3103-3110.
K_d	90 nM	J Med Chem. 2018;61(14):6350-6363.

Parameter	R848 single agent	Notes
Dose	0.02 mg/kg	J Hepatol. 2007;47(2):174-182.
C_{max}	7.5 ng / mL	J Hepatol. 2007;47(2):174-182.
AUC_{plasma}	45 ng hr / mL	J Hepatol. 2007;47(2):174-182.
$t_{1/2\ terminal}$	6.8 hr	J Hepatol. 2007;47(2):174-182.
K_d	30 nM	Theranostics. 2019;9(26):8426-8436.

	CANDI dual agent		
Parameter	**LCL-161**	**R848**	**Notes**
Dose	25 mg/kg	10 mg/kg	This paper
NP release rate $t_{1/2}$	6 hr	16 hr	This paper
NP $t_{1/2}$	8 hr		Approximated from NCT04843891
NP % ID/g tumor	~100		Approximated from intravital microscopy (this paper)
NP D_{eff}	$1x10^{-7}$ cm^2 s^{-1}		Approximated from albumin, see *Sci Adv*. 2022;8(17):eabl6339.
NP Permeability	$2x10^{-7}$ cm s^{-1}		Approximated from albumin, see *Sci Adv*. 2022;8(17):eabl6339.
Cellular NP uptake	0.007 min^{-1}		Fit to ID/g, this paper (intravital)